Methanol adsorption on the Si(100)-2 × 1 surface: a first-principles calculation

2005 J. Phys.: Condens. Matter 17 1289

(http://iopscience.iop.org/0953-8984/17/8/007)

INSTITUTE OF PHYSICS PUBLISHING JOURNAL OF PHYSICS: CONDENSED MATTER

J. Phys.: Condens. Matter **17** (2005) 1289–1300 doi:10.1088/0953-8984/17/8/007

Methanol adsorption on the Si(100)-2 × 1 surface: a first-principles calculation

Marilena Carbone[1] **and Karin Larsson**[2]

[1] Dipartimento di Scienze e Tecnologie Chimiche, Università 'Tor Vergata', Via della Ricerca Scientifica 1, 00133 Rome, Italy
[2] The Angstrom Laboratory, Department of Materials Chemistry, Box 538, 751 21 Uppsala, Sweden

Received 28 November 2004, in final form 4 January 2005
Published 11 February 2005
Online at stacks.iop.org/JPhysCM/17/1289

Abstract

The process of adsorption of methanol on a Si(100)-2 × 1 surface has been investigated theoretically, using density functional theory and a periodic boundary condition. The methanol adsorption on Si(100)-2 × 1 is known to be dissociative, resulting in hydrogen$_{(methanol)}$–oxygen$_{(surface)}$ and oxygen$_{(methanol)}$–silicon$_{(surface)}$ bond formation. Adsorption energies have been calculated here for five different surface sites for the methoxy fragment (top, bridge, cave, valley-bridge and pedestal). The top site was found to be energetically most favourable. Surface sites bridging Si atoms from the first and second atomic layers were found to be energetically equivalent to the top site. The effects of the position of the hydrogen fragment on the methoxy adsorption energy for the various adsorption sites were also investigated. These various hydrogen positions only influenced the adsorption energies marginally.

(Some figures in this article are in colour only in the electronic version)

1. Introduction

The adsorption of hydrocarbons on silicon surfaces has lately received more and more attention due to possible technological applications [1, 2]. Earlier studies of small molecules adsorbed on silicon surfaces with different orientations have given way to experimental and theoretical investigations including more and more complex adsorbates. The first experimental investigations included ethylene [3] and acetylene [4], and these were followed by successive adsorption studies involving adsorption of methanol [5], ethanol [6], phenol [7], *N*-methylpyrrole [8], toluene [9] and geranyl acetone [10]. The complexity of the molecules is counterbalanced by the different reactivities of the functional groups, which allows selective adsorption on different sites.

Theoretical investigations of hydrocarbon adsorption on Si(100) include studies performed at different levels of theory and cluster sizes representing the solid surface. The aim of such

studies is typically the description of favourable adsorption patterns and stable adsorption configurations.

Early studies were performed on small molecules such as acetylene [11, 12], ethylene [12] and propylene [13]. Later on, also ethylene hydrogen co-adsorption was investigated as a contribution to the debate on dimer breakage upon adsorption [14]. More recently, larger molecules as well as clusters have been employed. This gave rise to, for instance, investigation of methanol, formaldehyde, formic acid [15], methyl chloride [16], chlorobenzenes [17] and ethanol [18] adsorption on silicon.

Those studies give a wider picture of the adsorption process, including, for instance, the energetics of the process as a function of the reaction coordinate [15, 18].

In spite of the enormous effort and the large amount of studies, not all aspects of the adsorption process have been elucidated in any greater detail. In the present paper, we present a theoretical approach to one of those processes, with the main aim of obtaining a more complete picture of the adsorption process. The adsorption of methanol on Si(100)-2 $\times$ 1 has been thoroughly investigated by using density functional theory under periodic boundary conditions.

Earlier experimental investigations have dealt with methanol adsorption on the Si(100)-2 $\times$ 1 surface. Ehrley, Butz and Mantl used an epitaxially grown Si(100)-2 $\times$ 1 surface in studying the adsorption of methanol at 100 K, and its subsequent decomposition upon heating. Their infrared (IR) spectrum was attributed to a surface methoxy species adsorbed on Si(100) [19]. No decomposition of this surface intermediate was observed below 500 K, indicating a relatively high stability of the methoxy species. Glass, Wovchko and Yates used Fourier transform infrared spectroscopy (FTIR) to investigate the reaction of methanol with porous silicon and hydrogen passivated porous silicon [20]. At 300 K, methanol adsorbs onto hydrogen free porous silicon by cleavage of the O–H bond. Both of the resulting surface species (Si–H and Si–OCH_3) were determined as stable up to approximately 500 K.

Several photoemission and photodesorption experiments indicate that methanol dissociates upon adsorption on both Si(100)-2 $\times$ 1 and Si(111)-7 $\times$ 7. Valence band and Si 2p photoemission spectra show unequivocally that the O–H bond is broken and that two new bonds (a Si–O and a Si–H bond) are created. Furthermore, as far as Si(100)-2 $\times$ 1 is concerned, the surface dimers are involved in the adsorption process. In a first approach, it is natural to schematize the interaction with an atom of the dimer binding to the methoxy fragment and the other one to the hydrogen atom. A few general observations for adsorption of alcohols on silicon surfaces hint that the process might be more complex than described above. For instance, the quantitative analysis of the Si–O and Si–H related peaks is not always 1:1 as a function of surface coverage. There can be less hydrogen attached to the surface than expected (for ethanol adsorbed on Si(100)-2 $\times$ 1). Further fragmentation may occur upon large exposures to the adsorbate. This was observed for adsorption of both ethanol and methanol, on the Si(100)-2 $\times$ 1 and Si(111)-7 $\times$ 7 surfaces, respectively [5, 6b, 8].

A previous theoretical investigation on methanol adsorption on Si(100)-2 $\times$ 1 [15] indicates a readily dissociative adsorption giving rise to Si–OCH_3 and Si–H surface species. The reaction is barrierless, via a stable chemisorbed state and the transition state for dissociation. It is worth noting that a Si_9H_{12} cluster is used in this study. Its top layer consists of two Si atoms forming a silicon dimer only.

A complete picture of the dimer interaction with the dissociated methanol can be obtained by defining the adsorption site. The distribution of the surface dimers is such that the adsorption may occur on five different sites: top, bridge, valley-bridge, cave and pedestal (see figure 1). Depending on the adsorption energy, the adsorption of the methoxy fragment might be selective towards one or more of these sites. The present investigation aims at calculating the differences

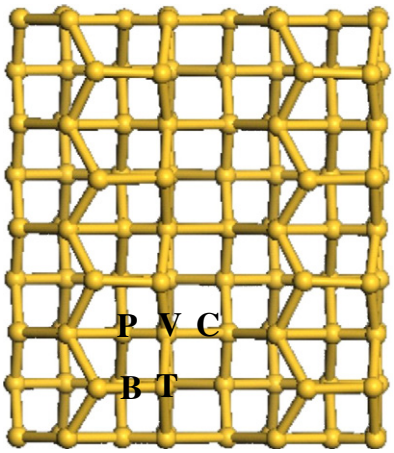

Figure 1. A schematic top view of Si(100) with the letters labelling various adsorption sites for the methoxy fragment (T for top, V for valley-bridge, C for cave, B for bridge and P for pedestal).

in adsorption energy for the five sites in order to establish (1) the existence of a preferential adsorption site, (2) eventual influences of the hydrogen position on the adsorption process and (3) the possibility of geometrical distortion (within the methoxy fragment) as a result of the adsorption.

2. Methods

The process of adsorption of methanol (CH_3OH) on Si(100)-2 × 1 has been investigated by means of first-principles calculations, using density functional theory (DFT) and the program package CASTEP from Accelrys, Inc. One of the most commonly applied approximations in DFT, the local density approximation (LDA) [21, 22], assumes the charge density to vary slowly on an atomic scale. The most important deficiency of the LDA method is that it does not have the correct asymptotic behaviour. Numerically, this leads to overestimation of the chemical bond energy in the system under investigation. A density gradient expansion is required to introduce inhomogeneity. Therefore, in the present study, exchange and correlation effects have been included within the generalized gradient approximation, GGA, developed by Perdew and Wang [23]. The pseudopotentials are generated by using the scheme of Lin *et al* [24] which ensures transferability of the potentials. The pseudopotentials are, then, used in the Kleinman–Bylander separable, norm-conserving form [25]. Moreover, the electronic wavefunctions were expanded in terms of plane waves with kinetic energy cut-offs up to 30 Ry and the electronic minimization was performed using a band-by-band conjugate gradient minimization technique [26].

The convergence criterion is the standard one provided by the program, i.e. 0.000 02 eV for the energy change per atom, 0.001 for the root mean square atomic displacement and 0.05 eV $Å^{-1}$ for the root mean square residual force on movable atoms.

The special **k**-points were generated by the Monkhorst–Pack scheme, which produces a uniform mesh of **k**-points in the reciprocal space [27]. The geometrical optimization was performed by using one special **k**-point in the irreducible wedge of the Brillouin zone for the (2 × 1) reconstruction, while for the final total energy calculations a mesh that gave eight special **k**-points was used. As a test, the total energy for a top site adsorption of CH_3O– was

calculated and compared by using various **k**-points. Four, eight and sixteen **k**-points (using the GGA method) resulted in a difference in total energy of 0.48 and 0.52 eV on comparing the results obtained using 4 and 8 **k**-points and 8 and 16 **k**-points, respectively. The fact that the difference in total energy when going from 8 to 16 **k**-points is only 0.04 eV, and that the present study focuses on differences in total energies of the order of 1 eV, makes the use of the lower accuracy (eight **k**-points) justified in the present investigation.

The calculations were performed under a periodic boundary condition with the periodically repeated unit cells referred to as super-cells. A surface model including six layers of Si atoms was included in this super-cell, with vacuum regions of about 8 Å in the (001) direction, while keeping the periodicity in the (100) and (010) directions (figure 1). The lower surface atoms in the slab were saturated with hydrogen atoms. All geometrical parameters of the surface layer of Si in the model, as well as the dissociated adsorbate, were allowed to fully relax. So also were the closest Si neighbours to the adsorbed H– fragments. The other atoms were fixed in order to hold the characteristics of the crystal.

3. Results and discussion

3.1. General

Previous experimental investigations concerning methanol (CH_3OH) adsorption on Si(100)-2×1 have indicated that the adsorption process occurs dissociatively, with O–H bond breakage within CH_3OH and subsequent Si–O bond formation between the surface and the CH_3O– fragment [5–7]. As a result of this dissociative adsorption process, two species are chemisorbed on the Si surface upon methanol adsorption: the CH_3O– and the H– fragments. The effect of various Si(100)-2×1 surface sites (top (T), valley-bridge (V), cave (C), bridge (B) and pedestal (P), as shown in figure 1) on the adsorption process of the methoxy (CH_3O–) fragment has been of a special interest in the present work. The purpose was not only to study the relative bond strengths for CH_3O– on these specific surface sites. The electronic and structural effect of the H– fragment position on the adsorption of CH_3O– fragments has also been of great interest. Hence, for each of the adsorption sites for the methoxy fragment, the H– fragment was positioned at various surface sites on Si(100)-2×1. The outcome of the calculations will be summarized and discussed in the following groupings:

(1) the adsorption site (determination of the most favourable adsorption site(s) for the methoxy fragment);
(2) the influence of H– on CH_3O– adsorption (the influence of the hydrogen position on the total energy for various methoxy sites);
(3) distortion of the methoxy fragment (the influence of adsorption on the geometry of the methoxy fragment).

3.2. The adsorption site

The calculations were performed by initially positioning the methoxy fragments on the various adsorption sites. The results (based on geometrical optimization procedures) that will be presented and discussed are here separated into three main groups (top site, valley-bridge/cave sites and bridge/pedestal sites), which differ mainly in the numerical value of the methoxy adsorption energy.

3.2.1. Top site. The calculated adsorption energies for the methoxy group are presented in table 1. The H– fragment (from the original methanol species) for all of these adsorptions was

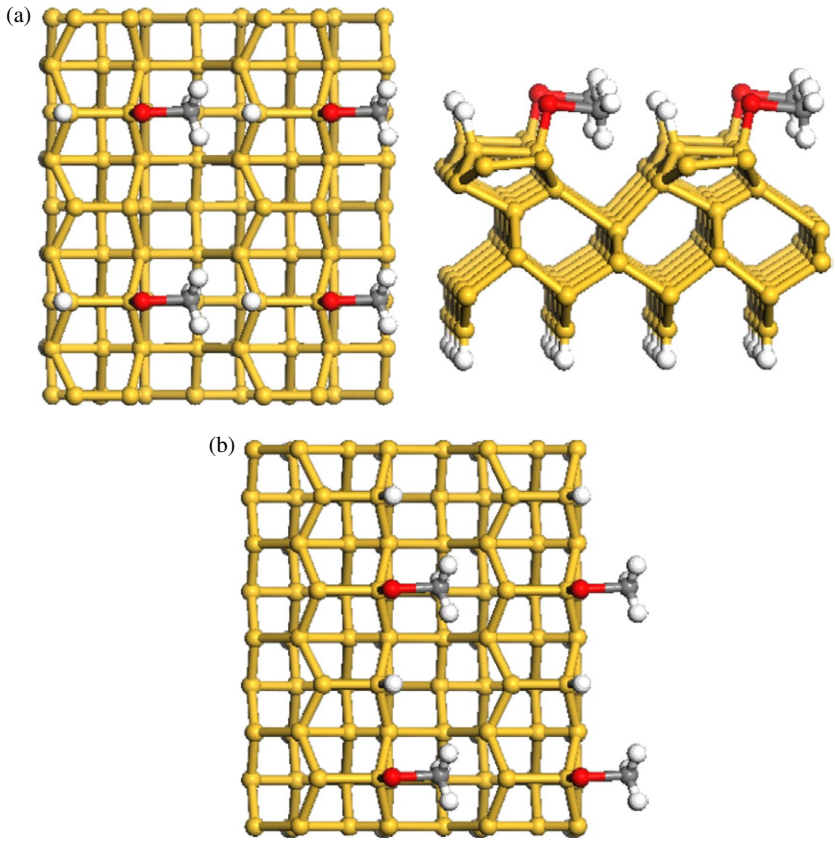

Figure 2. A schematic top view of the methoxy adsorption on the silicon top site. The two models (a) and (b) correspond to two different surface hydrogen positions. The methoxy fragment is completely bent towards the surface as a result of the adsorption. The total energies of the systems are reported in tables 1 and 2. In order to give a more representative picture of the resulting surface constitution; the model presented here contains four super-cells.

Table 1. Calculated adsorption energies for the methoxy adsorption on different surface sites. The numbers within parentheses at a specific surface site (e.g., top) correspond to the position of the hydrogen fragment closer to the methoxy fragment.

Model (1)	Adsorption energy (kJ mol^{-1})
Top (1)	668
Valley-bridge (1)	661
Cave (1)	645
Bridge (1)	574
Pedestal (1)	573

positioned on a neighbouring surface Si atom (as shown in figures 2–6). As can be seen in table 1, the top site was found to be the most energetically favourable adsorption site for the adsorption of CH_3O– on the Si(100)-2 × 1 surface. As a result of the geometrical optimization, the geometry of the adsorbed CH_3O– group was completely bent towards the silicon surface, with a $Si_{surface}$–O–C angle of 43.5° (see figure 2(a)). Moreover, the CH_3O– adsorbate was found

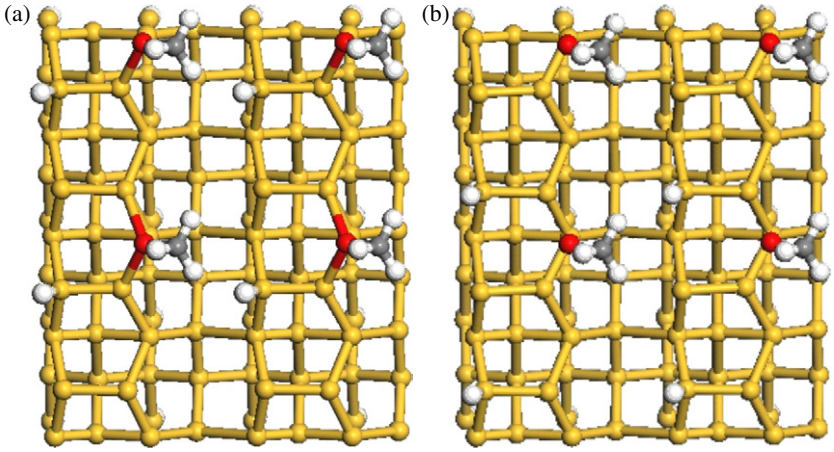

Figure 3. A schematic top view of the methoxy adsorption on the silicon valley-bridge site. As a result of the geometry optimization procedure, the final (equilibrium) position of the methoxy fragment has significantly shifted from the valley-bridge site to a position bridging between a top layer and a second-layer Si atom. The two models (a) and (b) correspond to two different surface hydrogen positions. The total energies of the systems are reported in tables 1 and 2.

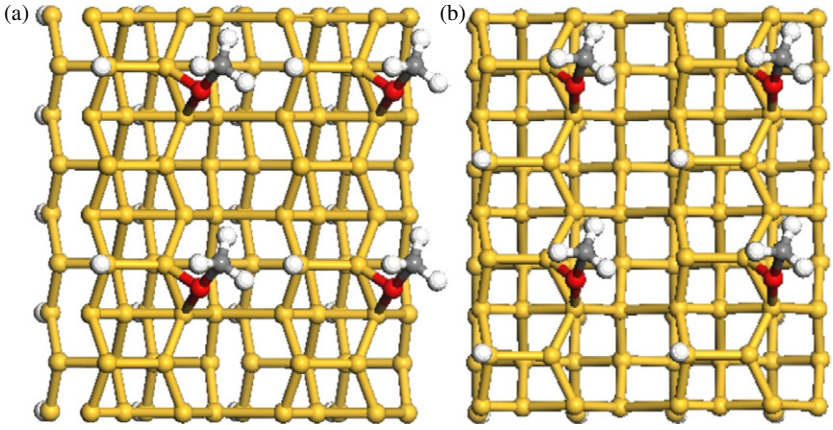

Figure 4. A schematic top view of the methoxy adsorption on the silicon cave site. The equilibrium position involves (similar to the situation with the valley-bridge site) a Si atom from the top layer and one from the second layer. The two models (a) and (b) correspond to two different surface hydrogen positions. The total energies of the systems are reported in tables 1 and 2.

to be bent towards the H– fragment which is attached to the closest neighbouring surface Si atom in a neighbouring dimer row.

The calculated Si–O and O–C bond distances of the Si–O–CH_3 moiety are 1.76 Å and 1.98 Å, respectively. Such values should be compared with the tabulated ones: 1.63 Å (Si–O, in SiO_2) and 1.43 Å (C–O single bond). The Si–O bond is only slightly elongated with respect to that of bulk silica, as could be expected for a surface bond. However, the C–O distance in the methoxy fragment is 38% longer than in free methanol molecules, which indicates a rather strong weakening of the C–O bond.

The top layer of the Si surface (and, hence, also the 2×1 reconstruction of the Si surface) was found to be largely geometrically preserved upon adsorption of CH_3O–.

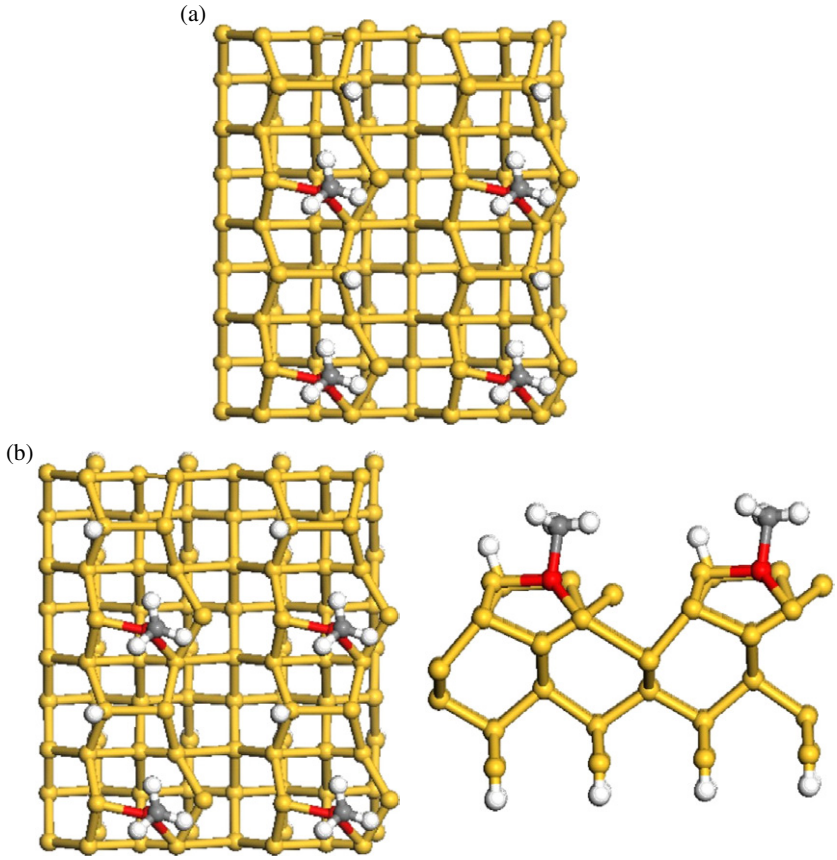

Figure 5. A schematic top view of the methoxy adsorption on the silicon bridge site. The two models (a) and (b) correspond to two different surface hydrogen positions. The total energies of the systems are reported in tables 1 and 2.

The adsorption of methanol on the top site is also the only case that can be compared with the previous investigation of Lu *et al* [15]. Since they use a single-dimer surface, this is also the only possible adsorption site that they can investigate. They find a Si–O bond distance of 1.678 Å and a C–O bond distance of 1.421 Å—hence much closer to the bulk silica and C–O tabulated single bonds respectively.

3.2.2. Valley-bridge and cave sites. When the methoxy fragment was initially positioned on the cave or valley-bridge sites (and thereafter allowed to geometrically relax), the adsorption energies obtained were numerically very similar to those in the situation with adsorption on a top site. They were only slightly smaller, by 23 and 14 kJ mol^{-1}, respectively. However, not only was the Si(100)-2 × 1 surface with CH_3O– adsorption initially on the valley-bridge and cave sites, respectively, energetically very similar to the situation with CH_3O– adsorption on a top site this was also, with one exception, the situation for the geometrical structure; also, the optimized geometry for the adsorbed CH_3O– group was, for these adsorption sites, completely bent towards the silicon surface, with a $Si_{surface}$–O–C angle of 62° versus 115°, and a $Si_{surface}$–$O_{adsorbate}$ bond distance of 2.25 versus 2.12 Å (see figures 3(a) and 4(a)). These bond distances are averaged ones, since O in the methoxy group binds to two Si atoms in the Si(100)-2 × 1

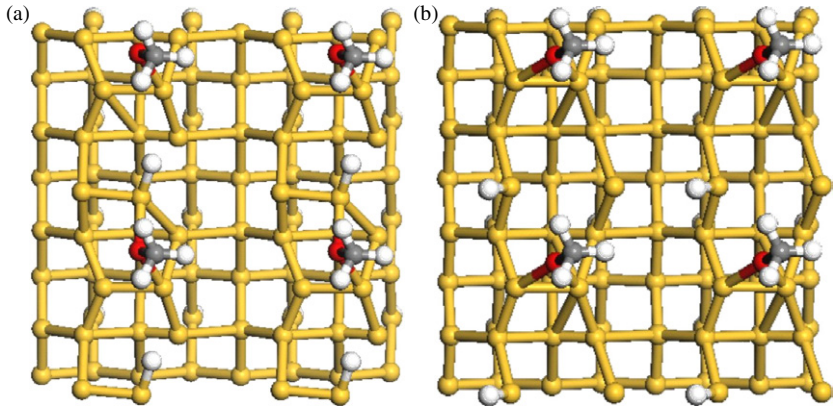

Figure 6. A schematic top view of the methoxy adsorption on the silicon pedestal site. The two models (a) and (b) correspond to two different surface hydrogen positions. The total energies of the systems are reported in tables 1 and 2.

surface. They are also longer than the corresponding Si–O bond for adsorption on a top site (a difference of 0.49 versus 0.36 Å), which usually indicates weaker adsorption bond energies. The corresponding O–C distances in the adsorbed CH_3O– fragment were both 2.00 Å, which is to be compared with the O–C distance for a top situation (1.98 Å). Hence, the intra-fragment bond weakening is even more pronounced for adsorption of CH_3O– to the valley-bridge and cave surface sites, respectively. Moreover, as can be seen in figures 3(a) and 4(a), there was also, for both of these different adsorption sites, a tendency for the CH_3O– adsorbate to bend towards a neighbouring H– fragment in the closest dimer row. The 2×1 reconstruction of the Si surface was found to be largely preserved upon CH_3O– adsorption for these adsorption sites too.

The main difference between the results for adsorption to a cave or valley-bridge site, compared to a top site, was the behaviour of CH_3O– during the geometrical optimization procedure. Neither the initial cave nor the valley-bridge site was found to represent any minimum on the energy potential surface for methoxy adsorption. The methoxy group was migrating from the original position (for both C and V sites) to an energy minimum situated further away (see figures 3(a) and 4(a)). These large displacements indicate that the final adsorption sites can no longer be defined as cave or valley-bridge. The reason for the displacement of CH_3O– from the original valley-bridge site (figure 3) is related to the nature of this site itself being an 'open' site. The interaction between the oxygen of the methoxy group and the silicon surface would be rather weak for the true valley-bridge site, since the methoxy group would, then, be positioned right above a Si atom within the third atomic layer. A much stronger adsorbate–surface interaction would be obtained either (i) by an inward movement of the CH_3O– group towards the Si surface, or (ii) by a movement towards the Si atoms within the surface top layer. As a test, several calculations were performed starting from slightly different positions of the methoxy group around the valley-bridge site. The final geometrical result presented in figure 3 was obtained for all initial positions used. The energy gain in the displacement from the valley-bridge to the final stable site was evaluated as the difference in total energy of the initial system and the system after geometrical optimization. It was found to be as large as 882 kJ mol^{-1}.

As can be seen in figure 4(a), the structural configuration obtained as a result of geometrical optimization when starting from a cave site is one where the methoxy group occupies a bridge

position between a Si atom in the surface atomic top layer and a Si atom in the second layer. The energy gain in the displacement from the initial position to the final stable site was found to be 304 kJ mol^{-1}. Due to the fact that equilibrium structural geometries and adsorption energies are very similar, the cave and valley-bridge sites can be defined as equivalent when considering this type of adsorption site.

3.2.3. Bridge and pedestal sites. When the methoxy fragment was initially positioned on the bridge or pedestal site, the calculated adsorption energy for the relaxed geometrical structure was significantly smaller compared to that for the adsorption on a top site. There was a difference in adsorption energy of 94 and 97 kJ mol^{-1}, respectively. These decreases in adsorption energies are correlated with expected bond elongations for the $Si_{surface}$–$O_{fragment}$ bonds: 2.22 (bridge site) and 2.21 (pedestal site) Å. However, no major difference of the O–C intra-fragment bond elongation was observed for these surface sites when compared to a top site (2.00 versus 2.03 Å). Hence, these adsorption sites showed even lower stabilities compared to the situations with initial positioning on valley-bridge and cave sites. The methoxy fragment initially adsorbed onto the bridge (or pedestal) surface site does not migrate to any top, or top-like, position during the geometrical optimization procedure.

However, a distortion of the silicon surface occurs that breaks the 2 × 1 symmetry. Prior to any geometrical optimization, the bridge site is characterized by a geometry where the oxygen atom of the methoxy fragment is bridging between the two atoms of a silicon dimer. The results obtained from the optimization procedure show that the methoxy fragment has moved towards the surface, with the effect of pushing away one of the dimer silicon atoms (figure 5(a)). The pedestal site is a position between two dimers. The results of the corresponding geometrical optimizations show a geometrical structure where the position of one of the silicon dimers is preserved, whilst the other one is distorted (figure 6(a)).

3.3. The influence of H– on CH_3O– adsorption

The influence of the various positions of the H– fragment on the adsorption processes of the methoxy fragment has also been included in the present study. Several starting positions of the hydrogen atoms were investigated for each of the methoxy fragment sites, but all of the geometrical optimizations lead to one of two possible final positions (as illustrated in parts (a) and (b) of each figure).

The calculated adsorption energies for the various adsorption sites are reported in table 1 (H– positioned closest to the CH_3O– adsorbate) and table 2 (H– positioned further away from the CH_3O– adsorbate). Firstly, the adsorption energy for a specific methoxy adsorption site, but for the two different hydrogen positions mentioned above, is to be compared in tables 1 and 2. The adsorption energy difference was found to be rather small. It never exceeds 20 kJ mol^{-1} for any of the CH_3O– sites investigated, and it is largest for the top site and smallest for the bridge one. It is worth noticing that the final adsorption geometry of the adsorbed methoxy fragment is almost identical, regardless of the hydrogen position (for every adsorption site studied). Hence, our results show that the position of the hydrogen fragment has only a minor influence on the adsorption energy, and no visible influence on the methoxy adsorption geometry. In particular, the energy difference for the two hydrogen adsorption sites is 20, 15, 9, 7 and 6 kJ mol^{-1} for the methoxy adsorption at top, cave, pedestal, valley-bridge and bridge methoxy sites, respectively.

In the different geometrical optimization procedures for the evaluation of the hydrogen effects, several hydrogen starting positions were used, including those on open sites, further away or closer to the methoxy fragments. In all cases studied, the final position for the

Table 2. Calculated adsorption energies for the methoxy adsorption on different surface sites. The numbers within parentheses at a specific surface site (e.g., top) correspond to the position of the hydrogen fragment further away from the methoxy fragment.

Model (2)	Adsorption energy (kJ mol^{-1})
Top (2)	648
Valley-bridge (2)	654
Cave (2)	630
Bridge (2)	568
Pedestal (2)	582

hydrogen atom was on top of a silicon atom. Each methoxy site is characterized by two possible final positions of the hydrogen atom, typically one closer and one slightly further away, which correspond to two different adsorption energies (and hence two local energy minima). In general, when the hydrogen is closer to the methoxy fragments the adsorption energy is more favourable. For the methoxy top site, the two hydrogen positions correspond to an adsorption process producing two fragments either on the same dimer (more favourable) or on two neighbouring dimers (less favourable). For cave and pedestal sites the situation is quite similar. If we consider the results of the geometrical optimization to yield top-like sites, the position of the hydrogen and methoxy fragment can be similarly described as on the same dimer (intra-dimer) or on neighbouring dimers (inter-dimer). Also, in those cases, the closer the hydrogen atom (favouring the intra-dimer case), the lower the energy.

The bridge and pedestal sites involve interaction of the methoxy adsorbate with one or two silicon dimers simultaneously. Therefore, no intra-dimer or inter-dimer adsorption can be defined. For the bridge site, the results of the geometrical optimizations for different hydrogen starting positions resulted in the adsorption of hydrogen on either of the silicon atoms within the neighbouring dimer. Given the distortion of the surface upon adsorption, those two sites are not equivalent and, also, in this case, the closer the hydrogen atom, the lower the adsorption energy (though the difference is only 6 kJ mol^{-1}). However, the situation is different for the pedestal site. The hydrogen fragment is adsorbed on either atom of the distorted dimer, and this results in a different geometrical distortion of the dimer. The adsorption energy difference in this case is 9 kJ mol^{-1}, but it is difficult to see how one can attribute this value to the hydrogen position rather than to the silicon surface distortion.

3.4. Distortion of the methoxy fragment

When adsorbed on the top site (energetically the most favourable one) the methoxy fragment has a final geometry bent towards the surface, with a Si–O–C angle close to 90°. This arrangement brings the methyl group closer to the surface, towards a chemical reaction distance. It was experimentally observed that high exposures of methanol (and ethanol) on silicon surfaces will result in further fragmentation of the methoxy fragment into oxygen and methyl [5–7] (or ethyl [8]). In the situation with a Si(100)-2 $\times$ 1 surface, such fragmentation may originate from a first fragmentation of the methanol into H– and an on-top adsorbed CH_3O– species, with a subsequent bending of CH_3O– towards the surface at a reaction distance. The activation of such a process at high exposures can be explained from the energetic aspect, provided that the release of energy from the incoming methanol molecules is high enough to overcome the energetic barrier to further fragmentation of previously adsorbed methanol fragments.

4. Conclusions

A theoretical investigation using the DFT method has been carried out in the study of the methanol adsorption process on the Si(100)-2 × 1 surface. Previous valence band and core-level photoemission studies of this system have shown that the adsorption of methanol is dissociative and that new Si–O and Si–H bonds are created upon adsorption. In the present investigation, five different adsorption sites have been considered for the adsorption process: top, bridge, valley-bridge, pedestal and cave sites. In addition, the presence of hydrogen species on different positions of the silicon surface was considered.

The geometrical optimization of the methoxy fragment adsorbed on different sites was found to lead to various adsorption energies (being measures of the stability of the adsorbate–substrate system). The adsorption sites can be divided into two groups: the top, cave and valley-bridge sites, on one hand, and the bridge and pedestal sites, on the other. Those two groups are separated by a 71–95 kJ mol^{-1} difference in adsorption energy. Distinctions can also be made within the subgroups. In the first energetically favoured group, the top site is the most stable one, and also the least geometrically distorted upon adsorption. The valley-bridge site is only slightly more energetically unfavourable, and the cave site has on average a 20 kJ mol^{-1} lower adsorption energy than the top site. However, the outputs of the geometrical optimizations of valley-bridge and pedestal sites are very similar to that for a top site. The bridge and pedestal surface sites are not only energetically less favoured, but also cause a higher degree of geometrical distortion.

The position of the hydrogen fragment has only a minor effect on the energy. Regardless of the starting position, it tends to migrate to an on-top site close to the methoxy fragment. For top and top-like methoxy adsorption sites, hydrogen tends to occupy preferentially a position on the same dimer as the methoxy fragment. For the bridge site, where both atoms of a silicon dimer are involved in the bond with the methoxy fragment, the preferred hydrogen position is on either of the silicon atoms of the neighbouring dimer. Also, in this case, the closer the methoxy and hydrogen fragments, the lower the adsorption energy of the methoxy group. For the pedestal site, the hydrogen position is associated with a surface distortion and the difference in energy might be related to either effect.

Finally, the geometrically distortion of the methoxy fragment towards the surface for a top adsorption obtained here may be the reason for the experimentally observed further fragmentation of methanol on the Si(100)-2 × 1 surface.

Acknowledgment

The calculations were performed using software programs from Accelrys (the first-principles calculations were done with the CASTEP program from the Cerius2 package).

References

[1] Dimitriadis E I, Girinoudi D, Thanailakis A and Georgoulas N 1995 *Semicond. Sci. Technol.* **10** 523
[2] Ikeda M, Inayoshi M and Hiraya A 1998 *J. Vac. Sci. Technol.* A **16** 2252
[3] Huang C, Widdra W and Weinberg W H 1994 *Surf. Sci.* **312** L953
[4a] Chu S-Y and Andersson A B 1988 *Surf. Sci.* **194** 55
[4b] Dyson A J and Smith P V 1997 *Surf. Sci.* **375** 45
[5] Carbone M, Piancastelli M N, Zanoni R, Comtet G, Dujardin G and Hellner L 1997 *Surf. Sci.* **390** 219
[6a] Eng J, Raghavachari K, Struck L M, Chabal Y J, Bent B E, Flynn G W, Christman S B, Chaban Ed E, Williams G P, Radermacher K and Mantl S 1997 *J. Chem. Phys.* **106** 9889
[6b] Carbone M, Piancastelli M N, Paggel J J, Weindel Chr and Horn K 1998 *Surf. Sci.* **412** 441

[7] Carbone M, Piancastelli M N, Casaletto M P, Zanoni R, Besnard-Ramage M J, Comtet G, Dujardin G and Hellner L 1999 *Surf. Sci.* **419** 114
[8] Tao F, Yuan Z L, Chen X F, Wang Z H, Dai Y J, Huang H G and Xu G Q 2003 *Phys. Rev.* B **67** 245406
[9] Carbone M, Piancastelli M N, Casaletto M P, Zanoni R, Comtet G, Dujardin G and Hellner L 2002 *Surf. Sci.* **498** 186
[10] Carbone M, Comtet G, Dujardin G, Hellner L and Mayne A J 2002 *J. Chem. Phys.* **117** 9606
[11] Toscano M and Russo N 1989 *J. Mol. Catal.* **55** 101
[12] Craig B I and Smith P V 1992 *Surf. Sci.* **276** 174
[13] Craig B I 1993 *Surf. Sci.* **298** 87
[14] Fisher A J, Blöchl P E and Briggs G A D 1997 *Surf. Sci.* **374** 298
[15] Lu X, Zhang Q and Lin M C 2001 *Phys. Chem. Chem. Phys.* **3** 2156
[16] Preuss M, Schmidt W G, Seino K and Bechstedt F 2004 *Appl. Surf. Sci.* **234** 155
[17] Naumkin F Y, Polanyi J C and Rogers D 2003 *Surf. Sci.* **547** 335
[18] Silvestrelli P L 2004 *Surf. Sci.* **552** 17
[19] Ehrley W, Butz R and Mantl S 1991 *Surf. Sci.* **248** 193
[20] Glass J A, Wovchko E A and Yates J T 1995 *Microcrystalline and Nanocrystalline Semiconductors* (*Materials Research Society Symp. Proc.* vol 358) (Pittsburgh, PA: Material Research Society) p 399
[21] Kleinman L and Bylander D M 1982 *Phys. Rev. Lett.* **48** 1425
[22] Teter M P, Payne M C and Allan D C 1989 *Phys. Rev.* B **40** 12255
[23] Perdew J P and Wang Y 1992 *Phys. Rev.* B **45** 13244
[24] Lin J S *et al* 1993 *Phys. Rev.* B **47** 4174
[25] Kleinman L and Bylander D M 1993 *Phys. Rev. Lett.* **48** 1425
[26] Hu P, King D A, Crampin S, Lee M-H and Payne M C 1994 *Chem. Phys. Lett.* **230** 501
[27] Monkhorst H J and Pack J D 1976 *Phys. Rev.* B **13** 5188